

1 **~~Ammonia~~Ammonium and nitrite oxidation in the upper euphotic zone of the**
2 **oligotrophic Red Sea**

3 Eyal Rahav^{1,2,3*}, Scott D Wankel⁴, and Adina Paytan²

4
5 ¹ Israel Oceanographic and Limnological Research, Haifa, Israel.

6 ² Institute of Marine Science, University of California, Santa Cruz, CA, USA.

7 ³ Department of Earth and Environmental Science, Ben-Gurion University of the Negev, Beer
8 Sheva, Israel.

9 ⁴ Marine Chemistry and Geochemistry Department, Woods Hole Oceanographic Institution,
10 Woods Hole, Massachusetts, USA.

11
12 *Corresponding author: eyrahav@ucsc.edu; eyal.rahav@ocean.org.il

13
14 **Abstract**

15 Nitrification is widely understood to be inhibited by light in the surface ocean, however,
16 increasing evidence indicates its occurrence at low levels at many sites. The extent to which
17 nitrification remains active in the euphotic zone could have important implications to new
18 production calculations, yet it remains understudied. Here, we quantified ~~ammonia~~ammonium
19 and nitrite oxidation rates in the euphotic zone of the Gulf of Aqaba (Northern Red Sea) from
20 late spring to late summer and examined environmental controls and implications for dark
21 carbon fixation (chemoautotrophy) and new production. Both ~~ammonia~~ammonium and nitrite
22 oxidation were detectable throughout the euphotic zone (~0.1-0.8 nmol N L⁻¹ d⁻¹). Overall,
23 rates were low in the highest-irradiance surface waters and increased with depth.~~Overall, rates~~
24 ~~increased with depth and were strongly suppressed in the highest irradiance surface waters.~~
25 Integrated rates over the entire euphotic zone (24-56 μmol N m⁻² d⁻¹) were among the lowest
26 reported for oligotrophic regions globally. This reflects extremely low substrate concentrations
27 and intense, though not complete, photo-inhibition. ~~Ammonia~~Ammonium and nitrite oxidation
28 together supported <2% of ~~chemoautotrophic activity~~dark carbon fixation rates, suggesting
29 other processes, not accounted for, ~~such as anaplerosis may be important~~drive this
30 chemoautotrophic activity. Depth-resolved correlations with environmental parameters
31 highlight light, temperature, and substrate availability as key regulators of both processes. Our
32 results show that nitrification in the Gulf of Aqaba operates at the lower bounds of global
33 euphotic zone rates and is loosely coupled to carbon cycling. These findings underscore the

34 need to better resolve nitrification dynamics in ultra-oligotrophic, rapidly warming, seas to
35 refine estimates of new production and chemoautotrophic carbon assimilation under future
36 ocean conditions.

37

38 **Key words:** Ammonia oxidation, Nitrite oxidation, Dark carbon fixation, Red Sea,
39 Oligotrophic.

40

41 **1 Introduction**

42 Nitrification, the sequential oxidation of ~~ammonia~~ammonium (NH_4^+) to nitrite (NO_2^-)
43 followed by the oxidation of nitrite to nitrate (NO_3^-), is a microbially mediated process central
44 to the regulation of nitrogen availability across nearly all aquatic environments, linking the
45 most reduced and oxidized states of nitrogen (Ward, 2008). Although nitrification does not
46 change the absolute inventory of bioavailable nitrogen (N) in the oceans, it alters the balance
47 among nitrogen N-species that serve as substrates for different organisms, thereby affecting
48 phytoplankton species abundance and growth (Fawcett et al., 2011). Ammonia oxidation is
49 carried out by ammonia-oxidizing archaea and bacteria (Francis et al., 2005; Wuchter et al.,
50 2006), while nitrite oxidation is performed by nitrite-oxidizing bacteria (Mincer et al., 2007;
51 Pachiadaki et al., 2017). Ammonia-oxidizing bacteria that perform the entire process have also
52 been identified in freshwater, terrestrial, and coastal habitats, but have not yet been found in
53 the open ocean (Daims et al., 2015; Fei et al., 2018; van Kessel et al., 2015).

54 Nitrification has been investigated across a wide range of marine settings, including the
55 Atlantic (Clark et al., 2008, 2022), the Pacific (Wan et al., 2021; Wankel et al., 2007), and the
56 Polar (Mdutyana et al., 2020; Shiozaki et al., 2019) ocean basins, as well as numerous coastal
57 and estuarine systems (Henriksen and Kemp, 1988; Herbert, 1999; Zhu et al., 2018). As a
58 chemoautotrophic process, nitrification contributes to organic carbon production in the ocean
59 interior (Middelburg, 2011; Pachiadaki et al., 2017), and may fuel bacterial carbon demand and
60 support heterotrophic food-webs in the mesopelagic and bathypelagic water depths. ~~(Bayer et~~
61 ~~al., 2024)~~(Bayer et al., 2025). The activity of nitrifiers is known to be promoted or inhibited by
62 many environmental factors (Ward, 2008), yet specific controls on its occurrence in the water
63 column and broader ecological implications across different ocean settings remain poorly
64 constrained (Tang et al., 2023). Additionally, because uptake of NH_4^+ and NO_3^- has long served
65 to differentiate between 'regenerated' and 'new' production, respectively (Eppley and Peterson,

66 1979), *in situ* production of NO_3^- by nitrification in the photic zone skews global estimates of
67 new production and carbon export in the oceans (Yool et al., 2007; Wankel et al., 2007).

68 Here, we report ~~ammonia~~ammonium and nitrite oxidation rates in the upper euphotic
69 zone (surface and down to ~100 m, representing 100% to ~0.5-1.8% of surface irradiance,
70 respectively) of the Gulf of Aqaba (GoA, Northern Red Sea) during late spring and throughout
71 the summer season. Rates were compared with common environmental physiochemical and
72 biological parameters to assess drivers of nitrification in this marine setting. Using these data,
73 we provide estimates of the contribution of ~~ammonia~~ammonium and nitrite oxidation to dark
74 carbon fixation (DCF) and new production in ~~this-thr~~ oligotrophic, warm and well-lit
75 systemGoA.

76 **2 Material and methods**

77 Seawater was collected every 20 m throughout the euphotic zone (0-100 m depth) at an
78 offshore, routinely monitored, station in the GoA (“Station A”, latitude 29.47 N, longitude
79 34.92 E). ~~Ammonia~~Ammonium and nitrite oxidation rates were assessed using stable ^{15}N
80 isotope enrichment incubations. Five monthly sampling events were performed spanning late
81 spring/early summer (May) to late summer (September) in 2023, covering the period in which
82 the GoA is characterized by oligotrophic N-poor conditions (Fuller et al., 2005; Mackey et al.,
83 2007). Ancillary water column measurements included temperature, salinity, photosynthetic
84 active radiation (PAR) (Seabird 19 Plus), inorganic nitrogen species concentrations (NO_2^- ,
85 NO_3^- , NH_4^+), chlorophyll-*a*, and rates of photosynthesis and ~~dark inorganic carbon fixation~~
86 ~~(DCF)~~.

87 **2.1 Inorganic nitrogen species**

88 Duplicate water samples for nitrite (NO_2^-) and nitrate (NO_3^-) were collected in 15 ml
89 acid-clean polyethylene tubes directly from Niskin bottles. Prior to filling, the tube was
90 thoroughly rinsed three times with sample water. After collection, samples were stored at 4 °C
91 in the dark and analyzed the following day. Nitrite (NO_2^-) and nitrate (NO_3^-) concentrations
92 were determined colorimetrically following standard procedures (Grasshoff et al., 1999).
93 Nitrite was measured directly using the Griess reaction, in which nitrite forms an azo dye after
94 reaction with sulfanilamide and N-(1-naphthyl)ethylenediamine and is quantified
95 spectrophotometrically ($\lambda=520$ nm). Nitrate was reduced to nitrite using a copper-coated
96 cadmium reduction column and subsequently ~~NO_2^- nitrate + NO_3^- nitrite~~ was analyzed by the
97 same azo-dye method. Nitrate concentrations were then calculated by difference. Analyses
98 were performed using a Flow Injection Autoanalyzer system (FIA, Lachat Instruments) (Model

99 QuikChem 8000). The analysis was automated, and peak areas were calibrated using standards
100 prepared in nutrient-deplete 0.2- μm filtered surface seawater from the GoA over a range of 0-
101 100 nmol L^{-1} . The detection limits were 10 nmol L^{-1} and 20 nmol L^{-1} for nitrite and nitrate,
102 respectively, with typical analytical precision of $\sim 20 \text{ nmol L}^{-1}$, consistent with previous
103 measurements in the GoA (e.g., Mackey et al., 2011).

104 Samples for ~~ammonia~~ammonium (NH_4^+) concentration were collected directly from
105 Niskin bottles into acid-washed plastic vials after rinsing 3 times with sample water. The
106 collected samples were stored in 4 °C in the dark and analyzed within an hour after collection.
107 ~~Ammonia~~Ammonium concentrations were determined using the orthophthaldialdehyde (OPA)
108 method (Holmes et al., 1999), where samples were first incubated with a working reagent of
109 OPA for 3 h and then measured fluorometrically (Turner Designs, Ex: 360 nm, Em: 420 nm).
110 The detection limit of the OPA analysis was $\sim 4 \text{ nmol L}^{-1}$ (Meeder et al., 2012).

111 Procedural blanks were routinely measured and subtracted from sample signals to
112 account for background contamination. Note that calibration and quality control procedures
113 were carried out during nutrient measurements. The analytical precision and detection limits
114 were within the expected range for oligotrophic seawater measurements.

115 2.2 ~~Ammonia~~Ammonium and nitrite oxidation rates

116 ~~Ammonia~~ Ammonium and nitrite oxidation rates were determined using stable isotope
117 tracer incubations (Beman et al., 2011; Bristow et al., 2015; Ward, 1987). Seawater was
118 collected into triplicate ~~0.51~~-L acid-cleaned transparent Nalgene bottles without headspace.
119 The bottles were incubated on land for 24 h in aquarium tanks continuously supplied with
120 running surface seawater, using neutral density screening nets simulating the light conditions
121 of the collection depth (no change in spectra). For ammonia oxidation, samples were amended
122 with ^{15}N -labeled ~~ammonium~~ammonium chloride ($^{15}\text{NH}_4\text{Cl}$, $>98 \text{ atom } \%$; Cambridge Isotope
123 Laboratories) at a concentration of $\sim 20 \text{ nmol L}^{-1}$ which is sufficient to yield a quantifiable
124 signal while potentially introducing some degree of tracer perturbation (discussed below)~~was~~
125 ~~expected to provide a quantifiable signal without substantially enhancing oxidation rates.~~ For
126 nitrite oxidation, samples were amended with $\sim 5 \text{ nmol L}^{-1}$ of ^{15}N -labeled sodium nitrite ($^{15}\text{NO}_2^-$
127 , $>98 \text{ atom } \%$), ~~again thus~~ minimally perturbing the *in situ* nitrite pool. At the end of the
128 incubation, subsamples were filtered onto a Supor 0.22 μm (47 mm) filter using gentle
129 filtration, and the filtrate ($<0.22 \mu\text{m}$) was kept frozen in the dark at $-20 \text{ }^\circ\text{C}$ until analysis. For
130 ammonia oxidation, the presence of $^{15}\text{NO}_2^-$ in the total dissolved nitrite pool was quantified by

131 isotope ratio mass spectrometry (IRMS) ~~after chemical conversion to N₂O using the azide~~
132 ~~method (Mellvin and Altabet, 2005).~~

133 -For nitrite oxidation, we quantified the ¹⁵NO₃⁻ in the dissolved nitrate pool after
134 conversion to nitrous oxide via the denitrifier method (Sigman et al., 2001) and subsequent
135 IRMS analysis. Note that in order to ensure sufficient nitrogen mass for isotopic analysis under
136 low ambient nutrient concentrations, relatively large incubation volumes (1 L) were used, and
137 a substantial fraction of the filtrate was processed for isotope measurements. The azide and
138 denitrifier methods employed here are well established for the analysis of low-concentration
139 nitrite and nitrate pools and allow reliable detection of ¹⁵N enrichment in oligotrophic systems
140 (Buchwald et al., 2018). Recent methodological modifications involving anion-exchange resin
141 enrichment coupled with azide reduction for low-concentration nitrite isotope analysis were
142 suggested to enhanced analytical sensitivity (Jiang et al., 2026); however, the established
143 approaches used here are widely applied in oligotrophic systems and were sufficient for robust
144 detection of ¹⁵N enrichment in the present study.

145 ~~Additionally, k~~Killed controls poisoned with HgCl₂ from each collection depth were
146 incubated in parallel to the experimental bottles to account for any abiotic transformations and
147 subtracted from the 'live' bottles. Rates in the 'mercury-killed' controls were typically
148 negligible relative to the 'live' bottles (usually <0.05 nmol N L⁻¹ d⁻¹). The resulting detection
149 limit, which was defined as the mean killed-control rate plus three standard deviations,
150 corresponded to 0.1 nmol N L⁻¹ d⁻¹. Rates below this threshold were considered
151 indistinguishable from background signal and were interpreted as 'below detection'.

152 Rates of ~~ammonia~~ammonium and nitrite oxidation were calculated following previous studies
153 (Beman et al., 2011; Bristow et al., 2015; Ward, 1987) as shown in ~~in~~Equations- 1-3:

154
155 (1) Ammonia oxidation =
$$\frac{\Delta (\text{atm}\% \text{ } ^{15}\text{N NO}_2) \times [\text{NO}_2]_{\text{final}}}{t \times F (\text{NH}_4)}$$

156
157 (2) Nitrite oxidation =
$$\frac{\Delta (\text{atm}\% \text{ } ^{15}\text{N NO}_3) \times [\text{NO}_3]_{\text{final}}}{t \times F (\text{NO}_2)}$$

158
159 (3) F substrate =
$$\frac{[^{15}\text{N substrate}]_{\text{added}}}{[\text{Substrate ambient}] + [\text{Substrate added}]}$$

160
161 Where, Δ(atm% ¹⁵N NO₂⁻) or Δ(atm% ¹⁵N NO₃⁻) = atom% excess ¹⁵N in the nitrite or nitrate
162 pool relative to natural abundance; [NO₂]_{final} or [NO₃]_{final} = final concentration of the nitrite

163 or nitrate pool (nmol L^{-1}); t = time (d); F_{NH_4} or F_{NO_2} = fractional ^{15}N enrichment of the
164 ~~ammonia~~ammonium or nitrite substrate pool.

165
166 Note that for the ammonia oxidation rates we added tracer additions which correspond
167 to 30-50% of the ambient NH_4^+ concentrations. While we aimed to minimize substrate
168 perturbation, such additions are inherently challenging in ultra-oligotrophic systems, where
169 even low absolute tracer concentrations can represent a substantial fraction of the ambient pool
170 (Zheng et al., 2020). Consequently, the reported rates should be considered as potential rates
171 under moderately enriched conditions rather than strictly *in situ* rates (Dodds and Jones, 1987).
172 Additionally, incubations were conducted over 24 h, which may allow for processes such as
173 ammonia regeneration, microbial turnover, and grazing to influence substrate availability and
174 isotopic dilution. Although HgCl_2 -poisoned controls and parallel measurements were used to
175 account for abiotic and background signals, these incubations cannot fully resolve short-term
176 dynamics or transient coupling between regeneration and oxidation processes. These
177 methodological constraints are inherent to low-rate measurements in oligotrophic systems
178 (Ward, 1985) and should be considered when interpreting the results. Another potential caveat
179 arising from the 24 h incubation is the potential production of unlabelled nitrite via
180 phytoplankton nitrate reduction (e.g., Travis et al., 2024) thereby diluting the $^{15}\text{NO}_2^-$ pool
181 leading to an underestimation of both ammonia and nitrite oxidation rates. In the present study,
182 however, primary production and ambient nitrite concentrations were low, suggesting that this
183 effect was likely limited in magnitude.

184

185 **2.3 Photosynthesis and Dark Carbon Fixation (DCF)**

186 Photosynthesis and chemoautotrophic DCF rates were measured using $\text{NaH}^{14}\text{CO}_3$
187 incorporation method (Steemann-Nielsen, 1952) with minor modifications (Reich et al., 2024,
188 2026). Triplicate seawater samples were collected from Niskin bottles in 50 ml acid-washed
189 falcon tubes and spiked with a diluted ‘working solution’ of $\text{NaH}^{14}\text{CO}_3$ (Perkin Elmer, specific
190 activity 56 mCi mmol^{-1}) at a final radioisotope dilution of $1:10^4$ v:v. Tubes were incubated in
191 the same tanks and under the same conditions used for the ~~ammonia~~ammonium and nitrite
192 oxidation measurements with one exception – the DCF bottles were first covered with
193 aluminum foil to prevent light penetration. The tubes were incubated for 24 h before being
194 filtered onto GF/F filters ($0.7 \mu\text{m}$ nominal pore size, 25 mm diameter) using low vacuum
195 pressure ($<50 \text{ mmHg}$). The filters were placed in glass scintillation vials and $50 \mu\text{l}$ of 37%
196 hydrochloric acid was added to remove the non-fixed ^{14}C -bicarbonate overnight. Scintillation

197 cocktail (5 ml, ULTIMA-GOLD) was then added to each vial and samples were counted using
198 a TRI-CARB 4810 TR (Packard) liquid scintillation counter. Additional T₀ blanks were
199 prepared by spiking bottles with NaH¹⁴CO₃ and filtering immediately (without incubation).
200 Blanks consistently yielded negligible activity. Added activity was measured by withdrawing
201 50 µl from ~~representative-random~~ spiked bottles (immediately after dosing and before
202 incubation) and adding it onto a new GF/F filter with 50 µl of ethanolamine (pH≈12) followed
203 by scintillation cocktail and counting immediately.

204 Photosynthesis was calculated as the difference between the disintegration per minute
205 (DPM) measured in the samples incubated under ambient irradiance and the dark bottles. DCF
206 and photosynthesis rates were calculated based on the Bermuda Atlantic Time-series Study
207 (BATS) protocol using the following Equation- 4:

$$208 (4) \text{ Production} = \frac{(DPM-blank)}{V} \times DIC \times \frac{AA \text{ vol}}{TDPM} \times f \times \frac{1}{t}$$

209 Where, DPM equals the disintegrations per minute, V = the filtered volume (50 ml), DIC is the
210 dissolved inorganic carbon in seawater (~25 mg C L⁻¹, similar to other oceanic sites, (Knap and
211 Michaels, 1993), AA vol = Added activity volume (50 µl), TDPM = Total ¹⁴C disintegration
212 per minute, t = incubation time (24h), and f = factor correcting isotope fractionation during
213 uptake of ¹⁴C (1.05).

214

215 **2.4 Chlorophyll.a analysis**

216 Seawater samples (250 ml) were filtered onto Whatman GF/F filters at low pressure
217 (<150 mbar), placed in glass vials and frozen in the dark at -20 °C. Chlorophyll.a was extracted
218 with 5 ml of cold acetone (90-%) overnight and determined by the non-acidification method
219 (Welschmeyer, 1994) using a Turner Designs (Trilogy) fluorometer.

220

221 **2.5 Statistical analysis**

222 Pairwise relationships between environmental variables and process rates were
223 evaluated using Pearson correlation coefficients calculated across all individual observations,
224 including all sampled depths (0-100 m) and stations. No prior averaging by depth or profile
225 was applied. Because many variables co-vary with depth and season, these correlations should
226 be interpreted as measures of co-variation rather than independent or causal relationships. Full
227 Pearson correlation statistics (r, r², p-values) are provided in Supplementary Tables S1 and S2.
228 Statistical analyses were performed using Python.

229

230 3 Results and discussion

231 3.1 Physiochemical and biological characteristics of the GoA during summertime

232 Sampling spanned from late spring (May) to the end of summer (September) within the
233 euphotic zone (0-100 m) of the GoA. Surface temperatures ranged from ~25 °C in May to ~28
234 °C at the end of summer (September) and declined to ~23.5 °C at 100 m during all sampling
235 events (Figure 1A). Photosynthetic active radiation (PAR) levels ranged from ~1200-1950
236 $\mu\text{mol quanta m}^{-2} \text{ s}^{-1}$ at the surface and decreased exponentially to ~10-20 $\mu\text{mol quanta m}^{-2} \text{ s}^{-1}$
237 at 100 m (Figure 1B), corresponding to 0.5-21.8% of the surface irradiation levels. The
238 corresponding diffuse attenuation coefficient (K_d) was ~0.03-0.04 m^{-1} , in agreement with
239 previous observations from the GoA (Dishon et al., 2012; Stambler, 2006) ~~and as well as in~~
240 other oligotrophic regimes (Stambler, 2012). Concentrations of NH_4^+ ranged from undetectable
241 to 65 nmol L^{-1} ~~without a clear vertical or temporal trend, except in May where surface~~
242 ~~concentrations were below detection~~ (Figure 1C). The corresponding integrated NH_4^+
243 inventory (0-100 m) was lowest in May (1.68 $\mu\text{mol m}^{-2}$) and highest in July (~4.57 $\mu\text{mol m}^{-2}$)
244 (Table 1). NO_2^- levels were generally low throughout the upper 100 m (from below detection
245 to <20 nmol L^{-1}), except in September when nitrite increased with depth reaching ~45 nmol L^{-1}
246 below 40 m (Figure 1D). Vertical NO_2^- profiles suggest active ammonia oxidation below the
247 strongly lit surface waters, especially during September, although we cannot rule out expulsion
248 of NO_2^- by phytoplankton under light limitation ~~(Ko et al., 2022)~~ (Berube et al., 2023; Collos,
249 1998). ~~Nevertheless, The~~ vertically integrated NO_2^- inventories ~~were generally low in all~~
250 ~~months examined, ranging~~ from 0.79-3.39 $\mu\text{mol m}^{-2}$ (Table 1). Surface NO_3^- was also low
251 (<20 nmol L^{-1}) and generally increased with depth, suggesting organic matter regeneration and
252 nitrification during summertime (Figure 1E), and/or that less NO_3^- is assimilated by
253 phytoplankton at deeper depths. The integrated NO_3^- inventory ranged from 2.65 $\mu\text{mol m}^{-2}$ in
254 May and September up to 10.36 $\mu\text{mol m}^{-2}$ in June (Table 1). ~~Taken together Collectively,~~ the
255 summertime inorganic N species concentrations in the upper 100 m were low, in agreement
256 with previous reports from the oligotrophic GoA (Mackey et al., 2011; Meeder et al., 2012;
257 Rahav et al., 2015). ~~The general increasing trend in NO_2^- and NO_3^- with depth and the nano-~~
258 ~~molar NH_4^+ levels suggest active nitrification below the well lit surface water that has not been~~
259 ~~previously quantified in the GoA.~~

260 ~~Phytoplankton biomass derived from eChlorophyll.a concentrations were~~ low in the
261 surface water (<0.15 $\mu\text{g L}^{-1}$) and gradually increased with depth reaching maximal values in
262 May and June (~0.60 $\mu\text{g L}^{-1}$) (Figure 2A). The corresponding integrated chlorophyll.a was 26-

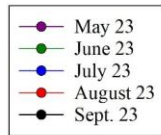
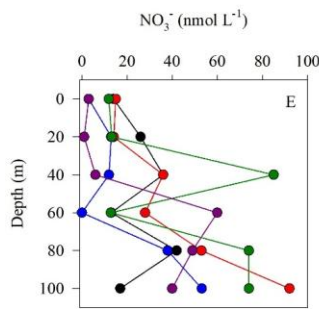
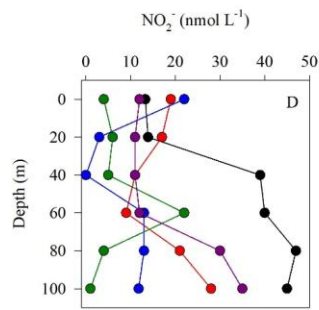
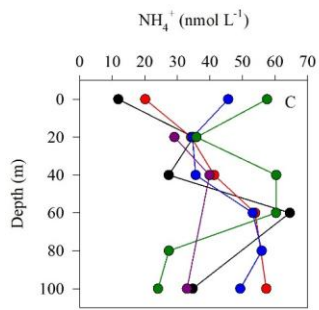
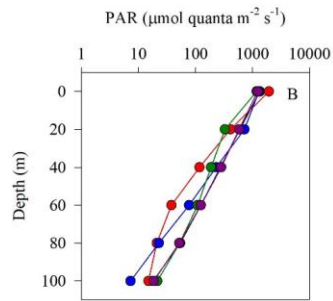
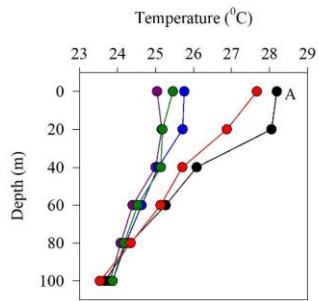
263 28 mg m⁻² except in August where it was 16 mg m⁻² (Table 1). As expected, photosynthesis
 264 rates were highest in the surface water and decreased with depth (Figure 2B), coinciding with
 265 the decreasing PAR levels (Figure 1B). Photosynthesis rates decreased from ~10 µg C L⁻¹ d⁻¹
 266 at the surface to below detection at 100 m, except in September when elevated rates were
 267 observed throughout the water column, ranging from ~10 to 25 µg C L⁻¹ d⁻¹ (Figure 2B). The
 268 resulting integrated photosynthesis rates ranged from 242 mg C m⁻² d⁻¹ in August to as high as
 269 1263 mg C m⁻² d⁻¹ in September (Table 1). Despite the fluctuation in photosynthetic rates
 270 between months, these values are within the range previously reported from the GoA (Rahav
 271 et al., 2015; Reich et al., 2024; Suggett et al., 2009).

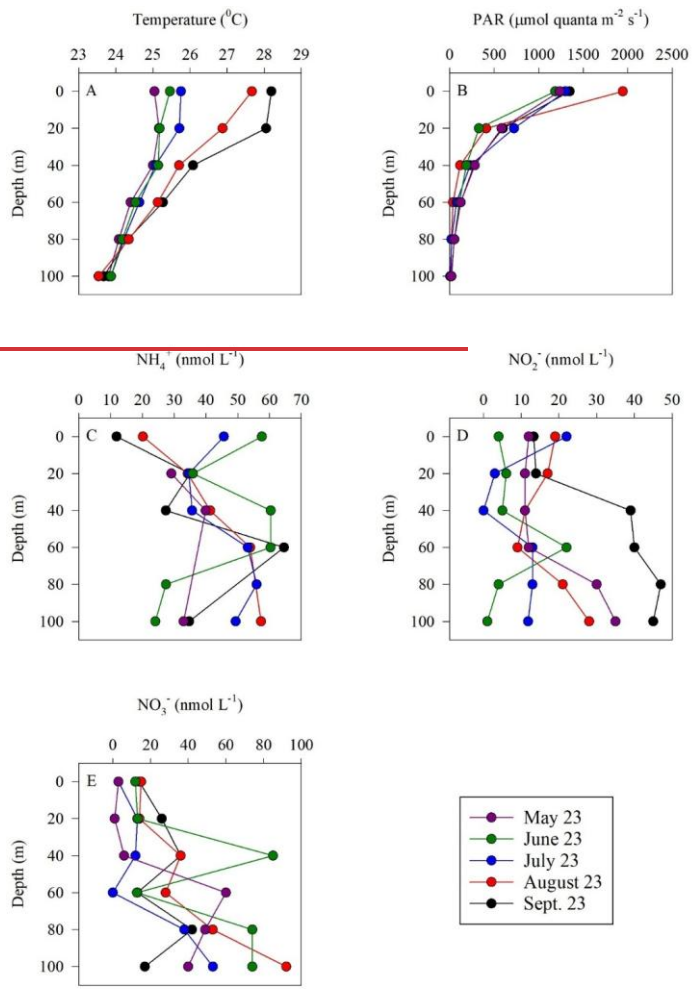
272 Chemoautotrophic DCF was lower than photosynthesis rates and exhibited no clear
 273 vertical trends (Figure 2C). The surface DCF ranged from ~0.2-0.6 µg C L⁻¹ d⁻¹ to ~0.1-0.9 µg
 274 C L⁻¹ d⁻¹ at 100 m (Figure 2C). The resulting integrated DCF ranged from 17-37 mg C m⁻² d⁻¹,
 275 in agreement with a recent study from the GoA (Reich et al., 2024), corresponding to ~3-10%
 276 of all the total autotrophic activity (photosynthesis ~~+~~and DCF ~~combined~~). While multiple
 277 microbial metabolisms involve chemoautotrophic carbon fixation, DCF is primarily attributed
 278 to ~~ammonia~~ammonium and nitrite oxidation, as these chemoautotrophic metabolisms are
 279 ubiquitous throughout the oxic water column (Middelburg, 2011; Tang et al., 2023). In general,
 280 ammonia oxidation likely provides energy that supports chemoautotrophic CO₂ assimilation
 281 throughout the euphotic zone. Though less energy efficient, nitrite oxidation also contributes
 282 to DCF and is considered especially relevant near the base of the euphotic zone where NO₂⁻
 283 often accumulates and reaches a maximum in concentration (Tang et al., 2023).

284
 285 **Table 1:** Summary of integrated values (0-100 m) measured in the GoA (N Red Sea) during
 286 summer 2023.

Variable	May 23	June 23	July 23	Aug. 23	Sept. 23
<u>Mixed layer depth (m)*</u>	45	31	21	15	28
NH ₄ ⁺ (µmol m ⁻²)	1.68	4.54	4.57	3.36	2.99
NO ₂ ⁻ (µmol m ⁻²)	1.76	0.79	0.94	1.64	3.39
NO ₃ ⁻ (µmol m ⁻²)	2.76	10.36	6.60	6.13	2.65
Chlorophyll.α (mg m ⁻²)	26	28	26	16	28
Photosynthesis (mg C m ⁻² d ⁻¹)	350	349	302	242	1263
DCF (mg C m ⁻² d ⁻¹)	32	17	35	27	37
NH ₄ ⁺ oxidation (µmol m ⁻² d ⁻¹)	28	48	39	45	56
NO ₂ ⁻ oxidation (µmol m ⁻² d ⁻¹)	24	38	45	39	44
Contribution of NH ₄ ⁺ oxidation to DCF (%)**	0.32	1.02	0.40	0.60	0.54
Contribution of NO ₂ ⁻ oxidation to DCF (%)***	0.05	0.13	0.08	0.09	0.07

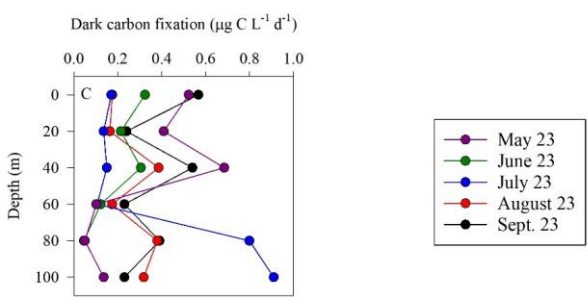
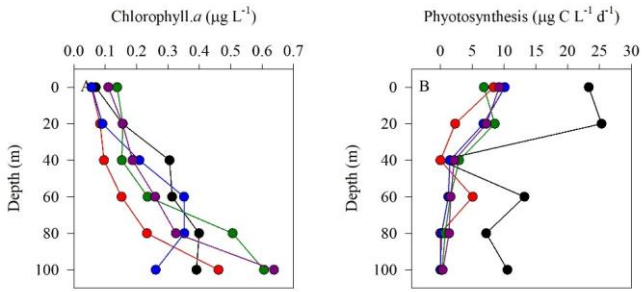
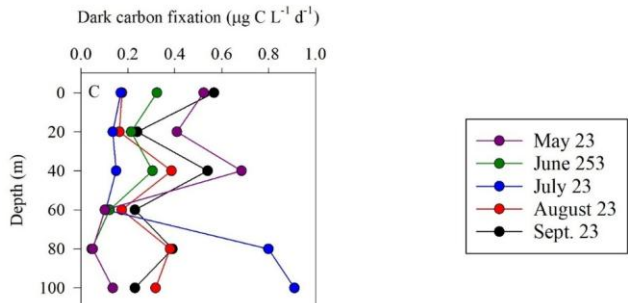
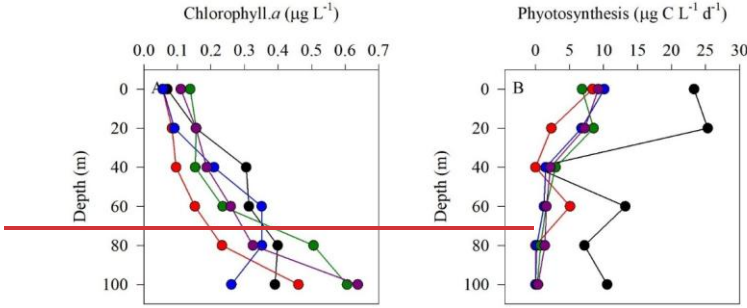
287 * Calculated from a temperature threshold criterion ($\Delta T = 0.2$ °C from surface values (de
288 Boyer Montégut et al., 2004).
289 **Assuming 0.3 moles of C fixed per mole of NH_4^+ oxidized (Santoro et al., 2010).
290 ***Assuming 0.05 moles of C per mole of NO_2^- oxidized (Beman et al., 2013).
291





293

294 **Figure 1:** Vertical distribution of temperature (A), PAR (B), NH_4^+ (C), NO_2^- (D) and NO_3^- (E)
 295 in the upper euphotic zone in the GoA, N Red Sea between May and September 2023.



296

297

298 **Figure 2:** Vertical distribution of chlorophyll-a (A), photosynthesis (B), and dark carbon
299 fixation (C) in the upper euphotic zone in the GoA, N Red Sea between May and September
300 2023.

301

302 3.2 Ammonia and nitrite oxidation rates

303 Ammonia and nitrite oxidation rates were generally low throughout the euphotic zone
304 yet exhibited an increasing trend with depth (Figure 3), consistent with regulation by light
305 inhibition. Overall, ammonia oxidation was homogeneous in the upper 40 m, ranging from
306 $\sim 0.10\text{-}0.55 \text{ nmol N L}^{-1} \text{ d}^{-1}$. Below this depth rates increased towards the bottom of the euphotic
307 zone ($\sim 100 \text{ m}$), ranging from $\sim 0.26\text{-}0.83 \text{ nmol N L}^{-1} \text{ d}^{-1}$ (Figure 3A,B). Ammonia oxidation
308 rates often reached a maximum near the base of the euphotic zone (below the 50-100 m layer)
309 as seen in other studies ([reviewed by](#) Tang et al., 2023). In general, these low euphotic zone
310 ammonia oxidation rates are consistent with light inhibition, given the high PAR of the GoA
311 during summer (Figure 1B, Wan et al., 2021). Competition of nitrifiers with phytoplankton for
312 NH_4^+ may also result in low ammonia oxidation rates, as has been reported in the surface sunlit
313 North Pacific (Smith et al., 2014). However, the highest integrated ammonia oxidation rate
314 (September, $56 \mu\text{mol m}^{-2} \text{ d}^{-1}$) was measured when chlorophyll.a levels and primary
315 productivity were also relatively high and similar to springtime when the lowest ammonia
316 oxidation rates were measured (May, $28 \mu\text{mol m}^{-2} \text{ d}^{-1}$) (Table 1). Thus, competition between
317 nitrifiers and phytoplankton for NH_4^+ does not appear to play a direct role in the regulation of
318 oxidation rates in our study. [That said, the lack of correlation between chlorophyll a and](#)
319 [ammonia \(\$R^2=0.003\$ \) does not preclude competition, but instead likely reflects rapid recycling](#)
320 [and tight coupling between ammonium production and uptake. This is further supported by the](#)
321 [lack of correlation between chlorophyll.a and ammonium \(\$r^2 = 0.003\$ \).](#) Ammonia oxidation
322 rates have also been shown to be influenced by trace metal availability, specifically iron and
323 copper (Martocello and Wankel, 2024; Shafiee et al., 2019, 2021). However, given the close
324 proximity to major deserts, iron is not considered a limiting factor for microbes in the surface
325 water of the GoA (Chen et al., 2008; Torfstein et al., 2017). The limiting factors for ammonia
326 oxidizers in the GoA should be further studied by simulating different nutrients and temperature
327 scenarios with or without amendments of an inhibitor of ammonia monooxygenase to better
328 examine controls on environmental rates ([Bayer et al., 2024](#))(Bayer et al., 2025).

329 [During the study period, the mixed layer depth shoaled from \$\sim 45 \text{ m}\$ in May to \$\sim 15 \text{ m}\$](#)
330 [in August \(Table 1\), reflecting progressive seasonal stratification. The vertical pattern of](#)
331 [ammonia oxidation \(Figure 3\) suggests that rates remained low throughout the strongly](#)

332 illuminated upper water column, while modest increases at 60–80 m likely reflected reduced
333 light inhibition and/or more favorable conditions for nitrifier activity below the mixed layer.
334 Thus, unlike systems where ammonia oxidation increases sharply below the deep chlorophyll
335 maximum, nitrification in the GoA appears to follow a more gradual depth-related response
336 during stratified conditions.

337 As with ammonia oxidation, rates of nitrite oxidation also increased with depth (Figure
338 3C,D). Nitrite oxidation ranged from 0.14 to 0.70 nmol L⁻¹ d⁻¹ (Figure 3C,D), with highest rates
339 measured over 80–100 m. Integrated nitrite oxidation rates were lowest in spring/early summer
340 (~24 μmol m⁻² d⁻¹) and increased between June to September (38–45 μmol m⁻² d⁻¹) (Table 1).
341 Nitrite oxidation maxima (~100 m) were deeper than those of ammonia oxidation (~60 m).
342 This vertical offset may reflect differences in substrate supply and the decoupling of ammonia
343 and nitrite oxidation along the water column in addition to differential sensitivity to light (Wan
344 et al., 2021). For example, ammonium supply may be more closely linked to shallower
345 regeneration processes, whereas nitrite can accumulate and persist at greater depths, which
346 may be related to the higher sensitivity of nitrite oxidizers to light (Wan et al., 2021)(Travis et
347 al., 2024).

348 Our results demonstrate that ammonia and nitrite oxidation occurred at comparable
349 rates, which is consistent with the typically low concentrations of NO₂⁻ observed in the GoA
350 during summertime (Figure 1D, Meeder et al., 2012), and consistent with the low net
351 accumulation of NO₂⁻ resulting from limited decoupling between the two steps of nitrification.
352 Converting photosynthesis to nitrogen demand using Redfield stoichiometry (C:N ≈ 6.6)
353 suggests that phytoplankton nitrogen requirements in surface waters may substantially exceed
354 the measured nitrification rates. This implies that regenerated nitrogen, including ammonium,
355 is rapidly consumed, potentially limiting its availability for ammonia-oxidizing
356 microorganisms. However, this inference is based on carbon-derived estimates of
357 phytoplankton demand rather than direct measurements of nitrogen uptake and should therefore
358 be interpreted cautiously. Nevertheless, previous studies indicate that ammonia uptake can
359 greatly exceed nitrification rates in oligotrophic surface waters (Mackey et al., 2011).

360 To assess substrate control, we examined the relationship between NH₄⁺ concentration
361 and ammonia oxidation rates across depths. This relationship was weak overall (Pearson,
362 r≈0.30), whereas rates were more strongly associated with depth (r≈0.75), indicating a
363 dominant role of depth-related gradients (Figure S1, Table S1). When examined by depth
364 intervals (0–50 m vs. 50–100 m), the NH₄⁺–oxidation relationship was weak in the upper 50 m
365 (r≈0.23) and stronger >50 m (r≈0.41) (Figure S1, Table S1). This suggests that rapid recycling

366 and competitive uptake weaken NH_4^+ oxidation rate coupling in surface waters, whereas
367 reduced light inhibition at depth allows a somewhat greater influence of NH_4^+ . These results
368 are consistent with previous studies showing that nitrification maxima are often decoupled
369 from NH_4^+ peaks and instead reflect depth-dependent ecological structuring (Beman et al.,
370 2012).

Field Code Changed

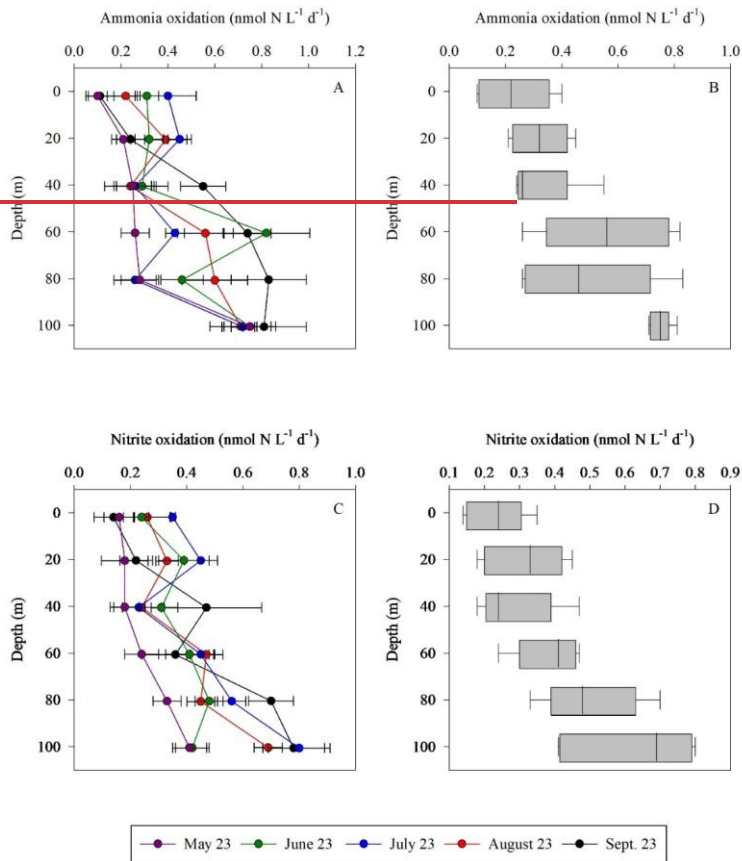
371 Note that a key consideration in interpreting the measured rates is the relative
372 magnitude of the $^{15}\text{NH}_4^+$ tracer addition compared to ambient substrate concentrations. In the
373 upper euphotic zone, where NH_4^+ concentrations were often near detection limits (Figure 1),
374 the addition of $\sim 20 \text{ nmol L}^{-1}$ (tracer) represented a substantial enrichment of the available pool.
375 Under such conditions, if ammonia oxidation were strongly substrate-limited, one might expect
376 a measurable stimulation of rates. However, the observed rates remained consistently low
377 across depths and sampling periods (Table 1; Figure 3), even under these 'enriched' conditions.
378 This suggests that factors other than immediate substrate availability exert primary control over
379 ammonia oxidation in the upper waters of the GoA. These may include low abundances of
380 ammonia-oxidizing archaea (Aizawa et al., 2023; Smith et al., 2016), strong light inhibition in
381 surface waters (Figure 1B), or physiological constraints associated with oligotrophic adaptation
382 (Yin et al., 2024; Zhou et al., 2024). Rather than indicating the absence of substrate limitation
383 *per se*, our results imply that ammonia oxidation operates under a combination of ecological
384 and environmental constraints that limit its overall contribution to nitrogen cycling in this
385 system. Moreover, the use of 24 h incubations introduce additional uncertainty, as internal
386 recycling of ammonium and microbial interactions may partially decouple measured rates from
387 instantaneous *in situ* conditions. Therefore, the rates reported here are interpreted as
388 conservative estimates of nitrification potential in the upper euphotic zone. Adding to that, in
389 oligotrophic systems, rapid recycling of dissolved inorganic nitrogen can influence both
390 substrate availability (Christie-Oleza et al., 2017) and isotopic enrichment during incubation
391 experiments (Stukel, 2020). Thus, processes such as ammonium regeneration and microbial
392 uptake may dilute the ^{15}N substrate pool or reduce accumulation of labelled products (Braun et
393 al., 2018). However, we surmise that any such processes, if occurred here, would tend to reduce
394 the apparent isotopic enrichment and thus bias rate estimates toward underestimation. Another
395 possible limitation regards the uncertainty in low nutrient concentrations in the GoA (most
396 notably within the upper mixed layer depth) that may propagate into rate calculations, as
397 substrate concentrations are explicitly included in the rate equations (see equations 1-3).
398 However, such uncertainty affects absolute rate estimates proportionally and does not alter the

399 overall interpretation of low nitrification activity. Accordingly, the reported rates should be
400 considered conservative estimates of nitrification activity over the incubation period.

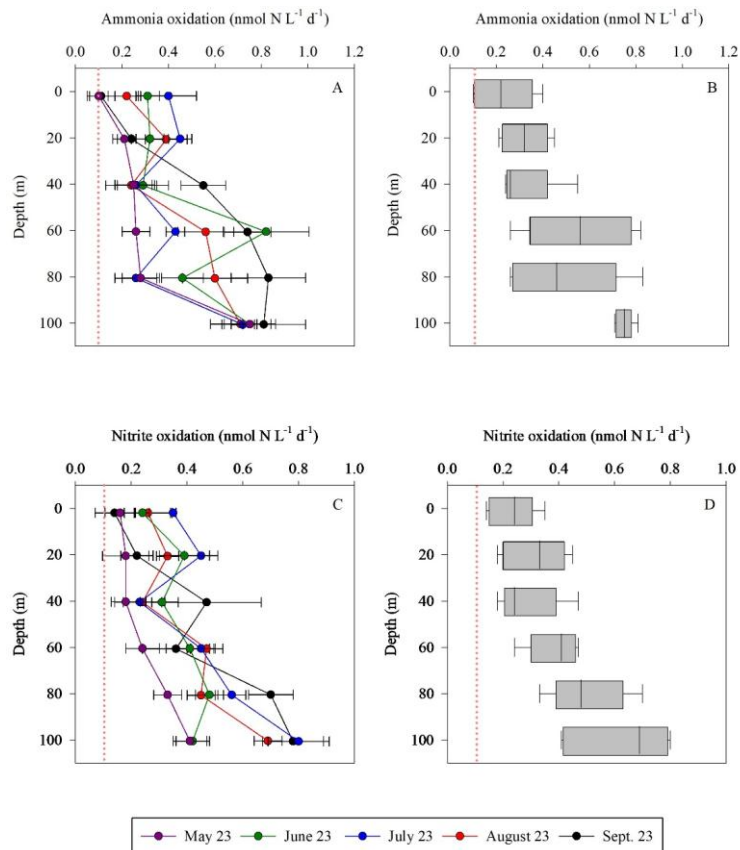
403 3.3 Contribution of ammonia and nitrite oxidation to DCF

404 DCF is widely thought to be dominated by ammonia and nitrite oxidation, as these
405 metabolic processes provide energy that, in turn, support chemoautotrophic CO₂ assimilation
406 (Middelburg, 2011), although additional pathways such as urea oxidation by ammonia
407 oxidizers may also contribute (Wan et al., 2024). While other chemoautotrophic metabolisms,
408 such as sulfur oxidation, anammox or methanotrophy also represent important drivers of
409 chemoautotrophy in some environments, these are unlikely to be relevant in the oxic,
410 oligotrophic waters of the GoA. DCF and nitrification are rarely measured simultaneously,
411 which prevents robust assessment of this relationship. Here, we explored DCF under the warm,
412 high-light, nutrient-poor conditions found in the GoA (Figure 1) and investigated how it relates
413 to corresponding rates of nitrification over the euphotic zone. We calculated the contribution
414 of ammonia and nitrite oxidation to DCF assuming 0.3 moles of C fixed per mole of NH₄[±]
415 (Santoro et al., 2010). Overall, the depth-integrated contribution of ammonia oxidation to DCF
416 ranged between 0-2%, consistent, yet often lower than reports from other oceanographic
417 settings. For example, ammonia oxidizers contributed only a small fraction to DCF in the
418 eastern tropical Pacific, accounting for <20% of depth-integrated rates (Bayer et al., 2025). The
419 depth-integrated contribution of nitrite oxidation to DCF was negligible, accounting for 0.05-
420 0.13% (Table 1). Thus, ammonia and nitrite oxidation together could account for only ~1% of
421 the DCF, lower than recent estimates from the eastern tropical Pacific (Bayer et al., 2025),
422 though similar to observations in culture experiments with ammonia oxidizers (Bayer et al.,
423 2023). It is notable, however, that relevant conversion factors between moles C fixed per mole
424 of N oxidized in the ocean should be better constrained (and may be site-specific) (Tang et al.,
425 2023), which could alter the calculated contribution discussed here. Nevertheless, we show that
426 ammonia and nitrite oxidation link N recycling with inorganic carbon assimilation in the
427 euphotic zone in the GoA, and while their contribution to total primary production is relatively
428 small, it may sustain part of the microbial metabolism in the nutrient-depleted surface waters
429 of the GoA. Our results suggest that other microbial metabolism processes (e.g., anaplerosis)
430 may also contribute to DCF in the GoA's euphotic zone and should be estimated separately in
431 future studies.

432 DCF in the sunlit ocean should not be interpreted solely as nitrification-driven
 433 chemoautotrophy. Even under dark incubation conditions, inorganic carbon fixation may
 434 include contributions from phytoplankton-associated dark metabolism, heterotrophic inorganic
 435 carbon assimilation, and other microbial pathways (Baltar and Herndl, 2019; Reich et al.,
 436 2026). A recent 10-year analysis from the GoA (same study site) showed that DCF is a
 437 persistent but variable component of carbon cycling, contributing substantially to total
 438 autotrophic carbon fixation (Reich et al., 2024). Therefore, while our data suggests that
 439 ammonia and nitrite oxidation contribute only a minor fraction of total DCF, the remaining
 440 DCF signal likely reflects multiple unresolved microbial processes (Reich et al., 2025).



441



442

443 **Figure 3:** Vertical distribution of ammonia oxidation (A,B) and nitrite oxidation (C,D) in the
 444 upper euphotic zone in the GoA, N Red Sea between May and September 2023. The Box
 445 Whisker plots sum the data distribution per depth (n=5). The pink dashed line signifies the
 446 detection limit.

447

448 3.3 Contribution of ammonia and nitrite oxidation to DCF

449 DCF is widely thought to be dominated by ammonia and nitrite oxidation, as these
 450 metabolic processes provide energy that, in turn, support chemoautotrophic CO₂ assimilation
 451 (Middelburg, 2011). While other chemoautotrophic metabolisms, such as sulfur oxidation,
 452 anammox or methanotrophy also represent important drivers of chemoautotrophy in some
 453 environments, these are unlikely to be relevant in the oxic, oligotrophic waters of the GoA.
 454 DCF and nitrification are rarely measured simultaneously, which prevents robust assessment
 455 of this relationship. To this end, we explored DCF under the warm, high light, nutrient poor

456 conditions found in the GoA (Figure 1) and how it relates to corresponding rates of nitrification
457 over the euphotic zone. We calculated the contribution of ammonia and nitrite oxidation to
458 DCF assuming 0.3 moles of C fixed per mole of NH_4^+ (Santoro et al., 2010). Overall, the depth-
459 integrated contribution of ammonia oxidation to DCF ranged between 0–2%, consistent, yet
460 often lower than reports from other oceanographic settings (Table 1). For example ammonia
461 oxidizers contributed only a small fraction to DCF in the eastern tropical Pacific, accounting
462 for <20% of depth integrated rates (Bayer et al., 2024). The depth integrated contribution of
463 nitrite oxidation to DCF was negligible, accounting for 0.05–0.13% (Table 1). Thus, ammonia
464 and nitrite oxidation together could account for only ~1% of the DCF, lower than recent
465 estimates from the eastern tropical Pacific (Bayer et al., 2024), though similar to observations
466 in culture experiments with ammonia oxidizers (Bayer et al., 2023). It is notable, however, that
467 relevant conversion factors between moles C fixed per mole of N oxidized in the ocean should
468 be better constrained (and may be site specific) (Tang et al., 2023), which could alter the
469 calculated contribution discussed here. Nevertheless, we show that ammonia and nitrite
470 oxidation link N recycling with inorganic carbon assimilation in the euphotic zone in the GoA,
471 and while their contribution to total primary production is relatively small (e.g., Figure 2), it
472 may sustain part of the microbial metabolism in the nutrient depleted surface waters of the
473 GoA. Our results also suggest that other microbial metabolism processes (e.g., anaplerosis)
474 may also contribute to DCF in the GoA's euphotic zone and should be estimated separately in
475 future studies.

477 3.4 Environmental drivers affecting ~~ammonia~~ammonium and nitrite oxidation

478 Nitrification is known to be affected by PAR, oxygen levels, temperature, nitrogen
479 substrate availability, pH, as well as by other environmental factors (Ward, 2008). Our results
480 are consistent overall with previous observations at other sites as both ~~ammonia~~ammonium and
481 nitrite oxidation rates linearly correlate with most of these environmental variables, either
482 positively or negatively (Figure 4; ~~Figure S1~~; ~~Tables S1 and S2~~). Most notably,
483 ~~ammonia~~ammonium and nitrite oxidation rates correlated with increasing depth and decreasing
484 PAR level, consistent with previous reports showing that light ~~has generally been found to~~
485 inhibit nitrifier growth and nitrification rates (Merbt et al., 2012; Olsen, 1989; Xu et al., 2019).
486 ~~Surprisingly,~~ Temperature correlated negatively with ~~ammonia~~ammonium and nitrite
487 oxidation rates (Figure 4, ~~$r=0.61$, $p<0.01$~~), likely reflects substrate limitation rather than a direct
488 ~~temperature effect~~. Previous studies showed that increasing temperature generally stimulates
489 nitrification by simultaneously altering substrate availability and enzyme kinetics (~~Emerson et~~

490 [al., 1975](#)). As temperature increases, the pKa of the NH_4^+ - NH_3 system decreases, shifting the
491 equilibrium toward NH_3 , the putative substrate of ammonia monooxygenase (Emerson et al.,
492 1975). In parallel, warming enhances enzymatic activity, accelerating the catalytic steps of both
493 ammonia and nitrite oxidation (Zheng et al., 2017, 2020). We surmise that in the stratified GoA,
494 warming strengthened stratification, enhanced photo_inhibition, and thereby increased
495 biological competition for ammonium, thus reducing substrate supply to nitrifiers despite
496 favorable enzyme kinetics, leading to the observed negative correlation between temperature
497 and nitrification. In agreement with this line of thought, substrate availability was positively
498 correlated with ammonia oxidation (NH_4^+ , NO_2^-) and nitrite oxidation (NO_2^- , NO_3^-),
499 highlighting the substrate-dependent nature of nitrification. Alternatively, these relationships
500 may reflect co-variation with depth and associated environmental gradients, rather than direct
501 substrate control alone (discussed below). Ammonia oxidation requires NH_4^+ or NH_3 as the
502 electron donor, while nitrite oxidation depends on NO_2^- availability. Elevated ambient
503 concentrations of these substrates make them more available to nitrifying enzymes, resulting
504 in higher reaction rates until enzymatic saturation or co-limitation with other nutrients are
505 reached (e.g., ~~trace metal, vitamins and other co-factors~~, PO_4^+). In oligotrophic systems such
506 as the GoA, where ambient NH_4^+ and NO_2^- concentrations are exceptionally low, even small
507 pulses of reduced or intermediate nitrogen (e.g., from organic matter remineralization, mixing,
508 or atmospheric deposition) may trigger an increase in nitrification rates.

509 Nitrification is generally expected to show a negative relationship with chlorophyll.a
510 in surface waters, where phytoplankton may compete with nitrifiers for reduced nitrogen
511 species. Consequently, most studies report suppressed ~~ammonia~~ammonium and nitrite
512 oxidation rates near the surface and enhanced rates below the chlorophyll maximum once light
513 levels decrease and substrate regeneration through organic matter remineralization becomes
514 more important (Beman et al., 2013; Yool et al., 2007). Here, however, we observed a positive
515 correlation between chlorophyll.a and ~~ammonia~~ammonium or nitrite oxidation (as well as with
516 photosynthesis, although not significantly). This pattern likely reflects conditions near ~~the~~
517 ~~can be explained by~~ the deep setting of the chlorophyll maximum (~80-100 m), where
518 chlorophyll a is elevated due to photo-acclimation under low light conditions rather than
519 strictly higher biomass (Cornec et al., 2021; Fennel and Boss, 2003; Scofield et al., 2020). In
520 these depths, reduced irradiance and enhanced organic matter turnover may promote
521 ammonium regeneration, providing substrate that supports nitrification~~where phytoplankton~~
522 ~~biomass is relatively high, but light is low and organic matter turnover is high, potentially~~
523 ~~providing regenerated NH_4^+ that fuels nitrification~~. These findings suggest that the expected

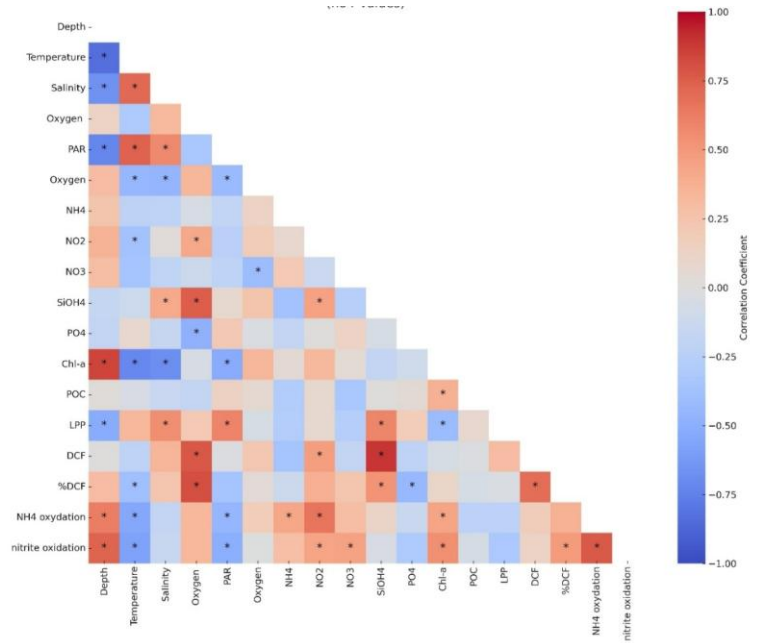
524 negative coupling at the surface is offset by strong regeneration and oxidation processes near
525 the deep chlorophyll maxima, resulting in an overall positive relationship when integrated
526 across the euphotic zone.

527 We expected that ~~ammonia~~ammonium and nitrite oxidation would show a significant
528 correlation with DCF (see discussion above). Nevertheless, although both ~~ammonia~~ammonium
529 and nitrite oxidation were positively coupled with DCF ($r=0.49$ and 0.17 , respectively), the
530 correlations were not statistically significant ($p>0.05$) and is in line with the overall low
531 contribution of these processes to DCF (discussion above and see Table 1). This suggests that
532 additional pathways such as anaplerotic processes may contribute to DCF (Dijkhuizen and
533 Harder, 1984; Erb, 2011), as well as other chemoautotrophic metabolisms beyond nitrification
534 such as urea oxidation, sulfur oxidation and iron oxidation (Arandia-Gorostidi et al., 2024;
535 Dang and Chen, 2017), while the contribution of ~~ammonia~~ammonium and nitrite oxidation to
536 total DCF is low (Table 1).

537 We note that correlation analysis should be interpreted with caution. Many parameters
538 considered here co-vary with depth (e.g., PAR, chlorophyll.*a*) and seasonal stratification
539 (mixed layer depth), which can produce strong apparent relationships without implying direct
540 mechanistic coupling. Furthermore, as the dataset is restricted to the upper 100 m, it does not
541 capture the full vertical structure of nitrification, including deeper maxima often observed
542 below the deep chlorophyll maximum. Accordingly, these correlations primarily reflect
543 processes operating within the upper euphotic zone and should not be extrapolated beyond this
544 depth range. Lastly, while variations in ammonia oxidation rates broadly co-occurred with
545 changes in primary production and chlorophyll *a*, these relationships should be interpreted with
546 caution. In this study, phytoplankton activity was assessed using carbon-based proxies, and no
547 direct measurements of nitrogen uptake or community composition were conducted. Therefore,
548 any inferred coupling between phytoplankton dynamics and nitrification remains indirect. The
549 observed patterns are consistent with the expectation that phytoplankton influence the
550 availability and cycling of regenerated nitrogen, but do not allow us to disentangle the relative
551 roles of substrate competition, regeneration, or microbial community structure. Future studies
552 that combine measurements of phytoplankton nitrogen demand, ammonium regeneration, and
553 nitrifier abundance and activity will be required to directly resolve these interactions in
554 oligotrophic systems.

555

556



557
 558 **Figure 4:** A heatmap showing Pearson correlation coefficients among measured environmental
 559 parameters and biogeochemical rates. Color shading indicates the strength and direction of the
 560 correlation. Asterisks denote statistically significant correlations ($p < 0.05$). [Full descriptive](#)
 561 [statistics for the correlations are provided in the Supplementary Tables S1 and S2.](#)

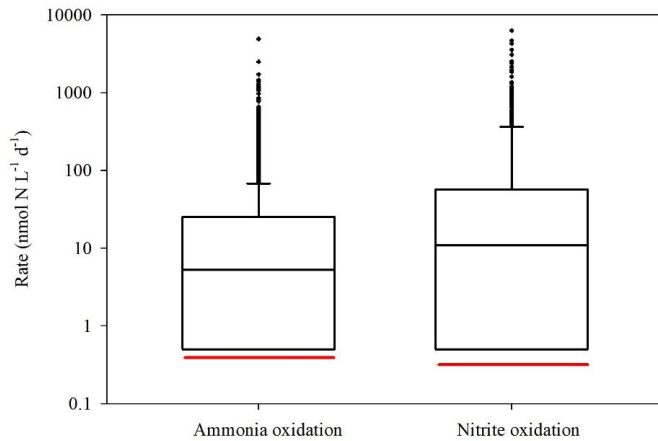
562

563 4 Conclusions

564 Globally, ~~ammonia~~ ammonium and nitrite oxidation rates in the euphotic zone span
 565 several orders of magnitude across offshore oceanic environments (Tang et al., 2023, Figure
 566 5). The rates we measured in the GoA during summer fall below these global medians (i.e., the
 567 red vs. black lines in Figure 5). The reason for the low rates in GoA is attributed to the low
 568 substrate availability during summertime (Figure 1C-E) but likely reflect a combination of
 569 environmental and ecological constraints rather than a single controlling factor. For example,
 570 the combination of high light intensity (Figure 1B) and penetration (i.e., $K_d \approx 0.04 \text{ m}^{-1}$) and
 571 enhanced stratification (Figure 1A) can further suppress nitrifier activity, either through
 572 photoinhibition of ammonia monooxygenase and/or by pushing microbial communities closer
 573 to their thermal tolerance limits. Moreover, the absence of measurements of nitrifier abundance
 574 preclude us from distinguishing whether low bulk rates reflect low population size or
 575 potentially high per-cell activity.

576 Additionally, while our results suggest a potential linkage between phytoplankton
577 activity and nitrogen cycling, this inference is based on carbon-derived proxies (primary
578 production and chlorophyll.a) rather than direct measurements of species-specific nitrogen
579 uptake or microbial community composition using genetic markers. Resolving this coupling
580 will require future studies that simultaneously quantify phytoplankton nitrogen demand,
581 ammonium regeneration, and nitrifier abundance and activity. Our results emphasize that
582 global compilations may be skewed toward more productive systems/seasons, and that
583 nitrification in extremely nutrient depleted regions may operate at lower rates and is tightly
584 coupled to local nitrogen cycling.

585 Future studies should focus on resolving the temporal and spatial variability of
586 nitrification rates and nitrifier communities in the context of ongoing climate change. This is
587 especially true for the GoA that experience rapid warming and ocean acidification. Long-term
588 time series and diel-scale observations are needed to capture seasonal, interannual, and daily
589 dynamics, particularly in relation to stratification, warming, and nutrient supply. Advanced
590 molecular approaches such as metagenomics, metatranscriptomics, and single-cell tools should
591 be applied to link community composition and functional potential with *in-situ* rate
592 measurements. Parallel measurements of trace metals will be essential to assess their role as
593 cofactors or inhibitors of key enzymes in ~~ammonia~~ammonium and nitrite oxidation.
594 Furthermore, the contribution of nitrification to DCF appears to be limited, suggesting that
595 additional microbial pathways contribute to inorganic carbon fixation in this system.
596 Constraining these contributions will require future studies that integrate rate measurements
597 with microbial community and metabolic analyses to better resolve the sources of DCF in
598 oligotrophic waters. Ultimately, combining high-resolution field observations with targeted
599 manipulations and modelling will improve our ability to predict how nitrification responds to
600 environmental change and contributes to current and future ocean nitrogen cycling.



601
 602 **Figure 5:** A literature compilation of reported euphotic zone's ammonia oxidation and nitrite
 603 oxidation recently reviewed Tang et al., (2023) and this study. The black line inside the boxes
 604 shows the median value of all studies considered, while the red line indicates the median values
 605 measured in the GoA during this study. Data include only offshore euphotic-zone
 606 measurements as defined in the original studies. We note that the depth and definition of the
 607 euphotic zone vary among regions, which may contribute to variability in reported rates.
 608

609 *Data availability.* All the data is presented in the graphs/table/text and will be made available
 610 in excel format upon request.

611 *Author contributions.* Conceptualized and conducted the field measurements; ER. Data
 612 curation, formal analysis, and visualization; ER, SDW and AP. The paper was prepared by ER,
 613 SDW and AP.

614 *Competing interests.* The contact author has declared that none of the authors has any
 615 competing interests.

616 *Acknowledgments.* The authors thank the personnel in the Inter University Institute for Marine
 617 Sciences in Eilat (IUI). This paper was supported by a grant from the Middle East Regional
 618 Cooperation (MERC) (M39-011) to ER and AP. We also thank the two anonymous reviewers
 619 for their constructive comments, which helped to significantly improve and refine the
 620 manuscript.

621

622

623 **References**

- 624 Aizawa, A., Watanabe, Y., Hashioka, K., Kadoya, A., Suzuki, S., Yoshimura, T., and Kudo,
625 I.: Contribution of ammonium oxidizing archaea and bacteria to intensive nitrification during
626 summer in Mutsu Bay, Japan, *Reg. Stud. Mar. Sci.*, 63, 102984,
627 <https://doi.org/https://doi.org/10.1016/j.rsma.2023.102984>, 2023.
- 628 Arandia-Gorostidi, N., Jaffè, A. L., Parada, A. E., Kapili, B. J., Casciotti, K. L., Salcedo, R.
629 S. R., Baumas, C. M. J., and Dekas, A. E.: Urea assimilation and oxidation support activity of
630 phylogenetically diverse microbial communities of the dark ocean, *ISME J.*, 18,
631 <https://doi.org/10.1093/ismejo/wrae230>, 2024.
- 632 Baltar, F. and Herndl, G.: Is dark carbon fixation relevant for oceanic primary production
633 estimates?, *Biogeosciences Discuss.*, 1–12, <https://doi.org/10.5194/bg-2019-223>, 2019.
- 634 Bayer, B., McBeain, K., Carlson, C. A., and Santoro, A. E.: Carbon content, carbon fixation
635 yield and dissolved organic carbon release from diverse marine nitrifiers, *Limnol. Oceanogr.*,
636 68, 84–96, <https://doi.org/https://doi.org/10.1002/lno.12252>, 2023.
- 637 Bayer, B., Kitzing, K., Paul, N. L., Albers, J. B., Saito, M. A., Wagner, M., Carlson, C. A.,
638 and Santoro, A. E.: Minor contribution of ammonia oxidizers to inorganic carbon fixation in
639 the ocean, *Nat. Geosci.*, 18, 1144–1151, <https://doi.org/10.1038/s41561-025-01798-x>, 2025.
- 640 Beman, J. M., Chow, C.-E., King, A. L., Feng, Y., Fuhrman, J. A., Andersson, A., Bates, N.
641 R., Popp, B. N., and Hutchins, D. A.: Global declines in oceanic nitrification rates as a
642 consequence of ocean acidification, *Proc. Natl. Acad. Sci.*, 108, 208–213,
643 <https://doi.org/10.1073/pnas.1011053108>, 2011.
- 644 Beman, J. M., Leilei Shih, J., and Popp, B. N.: Nitrite oxidation in the upper water column
645 and oxygen minimum zone of the eastern tropical North Pacific Ocean, *ISME J.*, 7, 2192–
646 2205, <https://doi.org/10.1038/ismej.2013.96>, 2013.
- 647 Berube, P. M., J., O. T., Anna, R., Trent, L., and W., C. S.: Production and cross-feeding of
648 nitrite within *Prochlorococcus* populations, *MBio*, 14, e01236-23,
649 <https://doi.org/10.1128/mbio.01236-23>, 2023.
- 650 de Boyer Montégut, C., Madec, G., Fischer, A. S., Lazar, A., and Iudicone, D.: Mixed layer
651 depth over the global ocean: An examination of profile data and a profile-based climatology,
652 *J. Geophys. Res. Ocean.*, 109, C12003, <https://doi.org/https://doi.org/10.1029/2004JC002378>,
653 2004.
- 654 Braun, J., Mooshammer, M., Wanek, W., Prommer, J., Walker, T. W. N., Rütting, T., and
655 Richter, A.: Full 15N tracer accounting to revisit major assumptions of 15N isotope pool
656 dilution approaches for gross nitrogen mineralization, *Soil Biol. Biochem.*, 117, 16–26,
657 <https://doi.org/https://doi.org/10.1016/j.soilbio.2017.11.005>, 2018.
- 658 Bristow, L. A., Sarode, N., Cartee, J., Caro-Quintero, A., Thamdrup, B., and Stewart, F. J.:
659 Biogeochemical and metagenomic analysis of nitrite accumulation in the Gulf of Mexico
660 hypoxic zone, *Limnol. Oceanogr.*, 60, 1733–1750,
661 <https://doi.org/https://doi.org/10.1002/lno.10130>, 2015.
- 662 Buchwald, C., Homola, K., Spivack, A. J., Estes, E. R., Murray, R. W., and Wankel, S. D.:
663 Isotopic constraints on nitrogen transformation rates in the deep sedimentary marine

664 biosphere, *Global Biogeochem. Cycles*, 32, 1688–1702,
665 <https://doi.org/https://doi.org/10.1029/2018GB005948>, 2018.

666 Chen, Y., Paytan, A., Chase, Z., Measures, C., Beck, A. J., Sañudo-Wilhelmy, S. A., and
667 Post, A. F.: Sources and fluxes of atmospheric trace elements to the Gulf of Aqaba, Red Sea,
668 *J. Geophys. Res. Atmos.*, 113, 1–13, <https://doi.org/10.1029/2007JD009110>, 2008.

669 Christie-Oleza, J. A., Sousoni, D., Lloyd, M., Armengaud, J., and Scanlan, D. J.: Nutrient
670 recycling facilitates long-term stability of marine microbial phototroph-heterotroph
671 interactions, *Nat. Microbiol.*, 2, 17100, <https://doi.org/10.1038/nmicrobiol.2017.100>, 2017.

672 Clark, D. R., Rees, A. P., and Joint, I.: Ammonium regeneration and nitrification rates in the
673 oligotrophic Atlantic Ocean: Implications for new production estimates, *Limnol. Oceanogr.*,
674 53, 52–62, <https://doi.org/https://doi.org/10.4319/lo.2008.53.1.0052>, 2008.

675 Clark, D. R., Rees, A. P., Ferrera, C. M., Al-moosawi, L., Somerfield, P. J., Harris, C.,
676 Quartly, G. D., Goult, S., Tarran, G., and Lessin, G.: Nitrite regeneration in the oligotrophic
677 Atlantic Ocean, *Biogeosciences*, 19, 1355–1376, <https://doi.org/https://doi.org/10.5194/bg-19-1355-2022>, 2022.

679 Collos, Y.: Nitrate uptake, nitrite release and uptake, and new production estimates, *Mar.*
680 *Ecol. Prog. Ser.*, 171, 293–301, 1998.

681 Cornec, M., Claustre, H., Mignot, A., Guidi, L., Lacour, L., Poteau, A., D’Ortenzio, F.,
682 Gentili, B., and Schmechtig, C.: Deep chlorophyll maxima in the global ocean: occurrences,
683 drivers and characteristics, *Glob. Biochem. cycles*, 35, e2020GB006759,
684 <https://doi.org/10.1029/2020GB006759>, 2021.

685 Daims, H., Lebedeva, E. V., Pjevac, P., Han, P., Herbold, C., Albertsen, M., Jehmlich, N.,
686 Palatinszky, M., Vierheilig, J., Bulaev, A., Kirkegaard, R. H., von Bergen, M., Rattei, T.,
687 Bendinger, B., Nielsen, P. H., and Wagner, M.: Complete nitrification by *Nitrospira* bacteria,
688 *Nature*, 528, 504–509, <https://doi.org/10.1038/nature16461>, 2015.

689 Dang, H. and Chen, C.-T. A.: Ecological energetic perspectives on responses of nitrogen-
690 transforming chemolithoautotrophic microbiota to changes in the marine environment, *Front.*
691 *Microbiol.*, 8, 1246, <https://doi.org/10.3389/fmicb.2017.01246>, 2017.

692 Dijkhuizen, L. and Harder, W.: Current views on the regulation of autotrophic carbon dioxide
693 fixation via the Calvin cycle in bacteria, *Antonie Van Leeuwenhoek*, 50, 473–487, 1984.

694 Dishon, G., Dubinsky, Z., Caras, T., Rahav, E., Bar-Zeev, E., Tzuber, Y., and Iluz, D.:
695 Optical habitats of ultraphytoplankton groups in the Gulf of Eilat (Aqaba), Northern Red Sea,
696 *Int. J. Remote Sens.*, 33, 2683–2705, <https://doi.org/10.1080/01431161.2011.619209>, 2012.

697 Dodds, W. K. and Jones, R. D.: Potential rates of nitrification and denitrification in an
698 oligotrophic freshwater sediment system, *Microb. Ecol.*, 14, 91–100, 1987.

699 Emerson, K., Russo, R. C., Lund, R. E., and Thurston, R. V.: Aqueous ammonia equilibrium
700 calculations: effect of pH and temperature, *J. Fish. Res. Board Canada*, 32, 2379–2383,
701 <https://doi.org/10.1139/f75-274>, 1975.

702 Eppley, R. W. and Peterson, B. J.: Particulate organic matter flux and planktonic new
703 production in the deep ocean, *Nature*, 282, 677–680, <https://doi.org/10.1038/282677a0>, 1979.

704 Erb, T. J.: Carboxylases in natural and synthetic microbial pathways,
705 <https://doi.org/10.1128/AEM.05702-11>, December 2011.

706 Fawcett, S. E., Lomas, M. W., Casey, J. R., Ward, B. B., and Sigman, D. M.: Assimilation of
707 upwelled nitrate by small eukaryotes in the Sargasso Sea, *Nat. Geosci.*, 4, 717–722,
708 <https://doi.org/10.1038/ngeo1265>, 2011.

709 Fei, X., Jian-Gong, W., Ting, Z., Bin, Z., Sung-Keun, R., and Zhe-Xue, Q.: Ubiquity and
710 diversity of complete ammonia oxidizers (Comammox), *Appl. Environ. Microbiol.*, 84,
711 e01390-18, <https://doi.org/10.1128/AEM.01390-18>, 2018.

712 Fennel, K. and Boss, E.: Subsurface maxima of phytoplankton and chlorophyll: Steady-state
713 solutions from a simple model, *Limnol. Oceanogr.*, 48, 1521–1534,
714 <https://doi.org/https://doi.org/10.4319/lo.2003.48.4.1521>, 2003.

715 Francis, C. A., Roberts, K. J., Beman, J. M., Santoro, A. E., and Oakley, B. B.: Ubiquity and
716 diversity of ammonia-oxidizing archaea in water columns and sediments of the ocean, *Proc.*
717 *Natl. Acad. Sci.*, 102, 14683–14688, <https://doi.org/10.1073/pnas.0506625102>, 2005.

718 Fuller, N. J., West, N. J., Marie, D., Yallop, M., Rivlin, T., Post, A. F., Interuniversity, T.,
719 Sciences, M., Beach, C., and Scanlan, D. J.: Dynamics of community structure and phosphate
720 status of picocyanobacterial populations in the Gulf of Aqaba , Red Sea, 50, 363–375, 2005.

721 Grasshoff, K., Kremling, K., and Ehrhardt, M.: *Methods of seawater analysis*, 3rd ed., edited
722 by: Kremling, K., Ehrenreich, I. M., and Grasshoff, K., Wiley, New York, 632 pp., 1999.

723 Henriksen, K. and Kemp, W. M.: Nitrification in estuarine and coastal marine sediments, in:
724 *Nitrogen Cycling in Coastal Marine Environments*, edited by: Blackburn, T. . and Sorensen,
725 J., John Wiley & Sons, Ltd, 207–249, 1988.

726 Herbert, R. A.: Nitrogen cycling in coastal marine ecosystems, *FEMS Microbiol. Rev.*, 23,
727 563–590, <https://doi.org/10.1111/j.1574-6976.1999.tb00414.x>, 1999.

728 Holms, R. ., Aminot, A., K erouel, R., Hooker, B. ., and Peterson, B. .: A simple and precise
729 method for measuring ammonium in marine and freshwater ecosystems, *Can. Data Rep. Fish.*
730 *Aquat. Sci.*, 56, 1801–1808, <https://doi.org/10.1139/cjfas-56-10-1801>, 1999.

731 Jiang, M., Koba, K., Ono, M., and Hayashi, K.: Improved isotopic analysis of low-
732 concentration freshwater nitrite by anion-exchange resin enrichment and azide reduction,
733 *Anal. Chem.*, 98, 2956–2967, <https://doi.org/10.1021/acs.analchem.5c05937>, 2026.

734 van Kessel, M. A. H. J., Speth, D. R., Albertsen, M., Nielsen, P. H., Op den Camp, H. J. M.,
735 Kartal, B., Jetten, M. S. M., and L ucker, S.: Complete nitrification by a single
736 microorganism, *Nature*, 528, 555–559, <https://doi.org/10.1038/nature16459>, 2015.

737 Mackey, K. R. M., Labiosa, R. G., Calhoun, M., Street, J. H., Post, A. F., and Paytan, A.:
738 Phosphorus availability, phytoplankton community dynamics, and taxon-specific phosphorus
739 status in the Gulf of Aqaba, Red Sea, *Limnol. Oceanogr.*, 52, 873–885,
740 <https://doi.org/10.4319/lo.2007.52.2.0873>, 2007.

741 Mackey, K. R. M., Bristow, L., Parks, D. R., Altabet, M. A., Post, A. F., and Paytan, A.: The
742 influence of light on nitrogen cycling and the primary nitrite maximum in a seasonally
743 stratified sea, *Prog. Oceanogr.*, 91, 545–560,
744 <https://doi.org/https://doi.org/10.1016/j.pocean.2011.09.001>, 2011.

745 Martocello, D. E. and Wankel, S. D.: Physiological influence of Fe and Cu availability on
746 nitrogen isotope fractionation during ammonia oxidation, *Environ. Sci. Technol.*, 58, 421–
747 431, <https://doi.org/10.1021/acs.est.3c05964>, 2024.

748 McIlvin, M. R. and Altabet, M. A.: Chemical conversion of nitrate and nitrite to nitrous oxide
749 for nitrogen and oxygen isotopic analysis in freshwater and seawater, *Anal. Chem.*, 77, 5589–
750 5595, <https://doi.org/10.1021/ac050528s>, 2005.

751 Mduyana, M., Thomalla, S. J., Philibert, R., Ward, B. B., and Fawcett, S. E.: The seasonal
752 cycle of nitrogen uptake and nitrification in the Atlantic sector of the Southern Ocean, *Global*
753 *Biogeochem. Cycles*, 34, e2019GB006363,
754 <https://doi.org/https://doi.org/10.1029/2019GB006363>, 2020.

755 Meeder, E., MacKey, K. R. M., Paytan, A., Shaked, Y., Iluz, D., Stambler, N., Rivlin, T.,
756 Post, A. F., and Lazar, B.: Nitrite dynamics in the open ocean-clues from seasonal and
757 diurnal variations, *Mar. Ecol. Prog. Ser.*, 453, 11–26, <https://doi.org/10.3354/meps09525>,
758 2012.

759 Merbt, S. N., Stahl, D. A., Casamayor, E. O., Martí, E., Nicol, G. W., and Prosser, J. I.:
760 Differential photoinhibition of bacterial and archaeal ammonia oxidation, *FEMS Microbiol.*
761 *Lett.*, 327, 41–46, <https://doi.org/10.1111/j.1574-6968.2011.02457.x>, 2012.

762 Michael Beman, J., Popp, B. N., and Alford, S. E.: Quantification of ammonia oxidation rates
763 and ammonia-oxidizing archaea and bacteria at high resolution in the Gulf of California and
764 eastern tropical North Pacific Ocean, *Limnol. Oceanogr.*, 57, 711–726,
765 <https://doi.org/https://doi.org/10.4319/lo.2012.57.3.0711>, 2012.

766 Middelburg, J. J.: Chemoautotrophy in the ocean, *Geophys. Res. Lett.*, 38, 94–97,
767 <https://doi.org/10.1029/2011GL049725>, 2011.

768 Mincer, T. J., Church, M. J., Taylor, L. T., Preston, C., Karl, D. M., and DeLong, E. F.:
769 Quantitative distribution of presumptive archaeal and bacterial nitrifiers in Monterey Bay and
770 the North Pacific Subtropical Gyre, *Environ. Microbiol.*, 9, 1162–1175,
771 <https://doi.org/https://doi.org/10.1111/j.1462-2920.2007.01239.x>, 2007.

772 Olsen, R.: Differential photoinhibition of marine nitrifying bacteria: a possible mechanism
773 for the formation of the primary nitrite maximum, *J. Mar. Syst.*, 31, 227–238, 1989.

774 Pachiadaki, M. G., Sintez, E., Bergauer, K., Brown, J. M., Record, N. R., Swan, B. K.,
775 Mathyer, M. E., Hallam, S. J., Lopez-Garcia, P., Takaki, Y., Nunoura, T., Woyke, T., Herndl,
776 G. J., and Stepanauskas, R.: Major role of nitrite-oxidizing bacteria in dark ocean carbon
777 fixation, *Science (80-.)*, 358, 1046–1051, <https://doi.org/10.1126/science.aan8260>, 2017.

778 Rahav, E., Herut, B., Mulholland, M. R., Belkin, N., Elifantz, H., and Berman-Frank, I.:
779 Heterotrophic and autotrophic contribution to dinitrogen fixation in the Gulf of Aqaba, *Mar.*
780 *Ecol. Prog. Ser.*, 522, 67–77, <https://doi.org/10.3354/meps11143>, 2015.

781 Reich, T., Belkin, N., Sisma-Ventura, G., Berman-Frank, I., and Rahav, E.: Significant dark
782 inorganic carbon fixation in the euphotic zone of an oligotrophic sea, *Limnol. Oceanogr.*,
783 9999, 1–14, <https://doi.org/10.1002/lno.12560>, 2024.

784 Reich, T., Belkin, N., Sisma-Ventura, G., Hauzer, H., Rubin-Blum, M., Berman-Frank, I.,
785 and Rahav, E.: Contribution of dark inorganic carbon fixation to bacterial carbon demand in
786 the oligotrophic Southeastern Mediterranean Sea, *Ocean Sci.*, 21, 3055–3067,
787 <https://doi.org/10.5194/os-21-3055-2025>, 2025.

788 Reich, T., Belkin, N., Sisma-ventura, G., Hauzer, H., Berman-frank, I., and Rahav, E.: Does
789 oligotrophy favor chemoautotrophy over photoautotrophy ?, *Prog. Oceanogr.*, 241, 103633,
790 <https://doi.org/10.1016/j.pocan.2025.103633>, 2026.

791 Santoro, A. E., Casciotti, K. L., and Francis, C. A.: Activity, abundance and diversity of
792 nitrifying archaea and bacteria in the central California current, *Environ. Microbiol.*, 12,
793 1989–2006, <https://doi.org/https://doi.org/10.1111/j.1462-2920.2010.02205.x>, 2010.

794 Scofield, A. E., Watkins, J. M., Osantowski, E., and Rudstam, L. G.: Deep chlorophyll
795 maxima across a trophic state gradient: A case study in the Laurentian Great Lakes., *Limnol.*
796 *Oceanogr.*, 65, 2460–2484, <https://doi.org/10.1002/lno.11464>, 2020.

797 Shafiee, R. T., Snow, J. T., Zhang, Q., and Rickaby, R. E. M.: Iron requirements and uptake
798 strategies of the globally abundant marine ammonia-oxidising archaeon, *Nitrosopumilus*
799 *maritimus* SCM1, *ISME J.*, 13, 2295–2305, <https://doi.org/10.1038/s41396-019-0434-8>,
800 2019.

801 Shafiee, R. T., Diver, P. J., Snow, J. T., Zhang, Q., and Rickaby, R. E. M.: Marine ammonia-
802 oxidising archaea and bacteria occupy distinct iron and copper niches, *ISME Commun.*, 1, 1,
803 <https://doi.org/10.1038/s43705-021-00001-7>, 2021.

804 Shiozaki, T., Ijichi, M., Fujiwara, A., Makabe, A., Nishino, S., Yoshikawa, C., and Harada,
805 N.: Factors regulating nitrification in the Arctic Ocean: potential impact of sea ice reduction
806 and ocean acidification, *Global Biogeochem. Cycles*, 33, 1085–1099,
807 <https://doi.org/https://doi.org/10.1029/2018GB006068>, 2019.

808 Sigman, D. M., Casciotti, K. L., Andreani, M., Barford, C., Galanter, M., and Böhlke, J. K.:
809 A bacterial method for the nitrogen isotopic analysis of nitrate in seawater and freshwater,
810 *Anal. Chem.*, 73, 4145–4153, <https://doi.org/10.1021/ac010088e>, 2001.

811 Smith, J. M., Damashek, J., Chavez, F. P., and Francis, C. A.: Factors influencing
812 nitrification rates and the abundance and transcriptional activity of ammonia-oxidizing
813 microorganisms in the dark northeast Pacific Ocean, *Limnol. Oceanogr.*, 61, 596–609,
814 <https://doi.org/https://doi.org/10.1002/lno.10235>, 2016.

815 Stambler, N.: Light and picophytoplankton in the Gulf of Eilat (Aqaba), *J. Geophys. Res.*,
816 111, C11009, 2006.

817 Stambler, N.: Underwater light field of the Mediterranean Sea, in: *Life in the Mediterranean*
818 *Sea: A Look at Habitat Changes*, edited by: Stambler, N., Nova Science Publishers, 1–739,
819 2012.

820 Steemann-Nielsen, E.: The use of radioactive carbon (¹⁴C) for measuring organic production
821 in the sea, *J. des Cons. Int. Pour Explor. la Mer*, 18, 117–140, 1952.

822 Stukel, M. R.: Investigating equations for measuring dissolved inorganic nutrient uptake in
823 oligotrophic conditions, *Limnol. Oceanogr. Methods*, 18, 656–672, 2020.

824 Suggett, D. J., Stambler, N., Prášil, O., Kolber, Z., Quigg, A., Vázquez-Domínguez, E.,
825 Zohary, T., Berman, T., Iluz, D., Levitan, O., Lawson, T., Meeder, E., Lazar, B., Bar-Zeev,
826 E., Medova, H., and Berman-Frank, I.: Nitrogen and phosphorus limitation of oceanic
827 microbial growth during spring in the Gulf of Aqaba, *Aquat. Microb. Ecol.*, 56, 227–239,
828 2009.

829 Tang, W., Ward, B. B., Beman, M., Bristow, L., Clark, D., Fawcett, S., Frey, C., Fripiat, F.,
830 Herndl, G. J., Mduyana, M., Paulot, F., Peng, X., Santoro, A. E., Shiozaki, T., Sintes, E.,
831 Stock, C., Sun, X., Wan, X. S., Xu, M. N., and Zhang, Y.: Database of nitrification and
832 nitrifiers in the global ocean, *Earth Sci. Rev.*, 15, 5039–5077,
833 <https://doi.org/https://doi.org/10.5194/essd-15-5039-2023>, 2023.

834 Torfstein, A., Teutsch, N., Tirosh, O., Shaked, Y., Rivlin, T., Zipori, A., Stein, M., Lazar, B.,
835 and Erel, Y.: Chemical characterization of atmospheric dust from a weekly time series in the
836 north Red Sea between 2006 and 2010, *Geochim. Cosmochim. Acta*, 211, 373–393,
837 <https://doi.org/10.1016/j.gca.2017.06.007>, 2017.

838 Travis, N. M., Kelly, C. L., and Casciotti, K. L.: Testing the influence of light on nitrite
839 cycling in the eastern tropical North Pacific, *Biogeosciences*, 21, 1985–2004,
840 <https://doi.org/10.5194/bg-21-1985-2024>, 2024.

841 Wan, X. S., Sheng, H.-X., Dai, M., Church, M. J., Zou, W., Li, X., Hutchins, D. A., Ward, B.
842 B., and Kao, S.-J.: Phytoplankton-nitrifier interactions control the geographic distribution of
843 nitrite in the upper ocean, *Global Biogeochem. Cycles*, 35, e2021GB007072,
844 <https://doi.org/https://doi.org/10.1029/2021GB007072>, 2021.

845 Wan, X. S., Sheng, H.-X., Shen, H., Zou, W., Tang, J.-M., Qin, W., Dai, M., Kao, S.-J., and
846 Ward, B. B.: Significance of Urea in Sustaining Nitrite Production by Ammonia Oxidizers in
847 the Oligotrophic Ocean, *Global Biogeochem. Cycles*, 38, e2023GB007996,
848 <https://doi.org/https://doi.org/10.1029/2023GB007996>, 2024.

849 Wankel, S. D., Kendall, C., Pennington, J. T., Chavez, F. P., and Paytan, A.: Nitrification in
850 the euphotic zone as evidenced by nitrate dual isotopic composition: Observations from
851 Monterey Bay, California, *Glob. Biochem. cycles*, 21, 1–13,
852 <https://doi.org/10.1029/2006GB002723>, 2007.

853 Ward, B. B.: Light and substrate concentration relationships with marine ammonium
854 assimilation and oxidation rates, *Mar. Chem.*, 16, 301–316,
855 [https://doi.org/https://doi.org/10.1016/0304-4203\(85\)90052-0](https://doi.org/https://doi.org/10.1016/0304-4203(85)90052-0), 1985.

856 Ward, B. B.: Nitrogen transformations in the Southern California Bight, *Deep Sea Res. Part*
857 *A. Oceanogr. Res. Pap.*, 34, 785–805, [https://doi.org/https://doi.org/10.1016/0198-](https://doi.org/https://doi.org/10.1016/0198-0149(87)90037-9)
858 [0149\(87\)90037-9](https://doi.org/https://doi.org/10.1016/0198-0149(87)90037-9), 1987.

859 Ward, B. B.: Nitrification in Marine Systems, in: *Nitrogen in the Marine Environment*
860 *Environment*, edited by: Capon, D. G., Bronk, D. A., Mulholland, M. R., and Carpenter, E.
861 J., Elsevier, 199–262, <https://doi.org/10.1016/B978-0-12-372522-6.00005-0>, 2008.

862 Welschmeyer, N. A.: Fluorometric analysis of chlorophyll a in the presence of chlorophyll b
863 and pheopigments, *Limnol. Oceanogr.*, 39, 1985–1992, 1994.

864 Wuchter, C., Abbas, B., Coolen, M. J. L., Herfort, L., van Bleijswijk, J., Timmers, P., Strous,
865 M., Teira, E., Herndl, G. J., Middelburg, J. J., Schouten, S., and Sinninghe Damsté, J. S.:
866 Archaeal nitrification in the ocean, *Proc. Natl. Acad. Sci.*, 103, 12317–12322,
867 <https://doi.org/10.1073/pnas.0600756103>, 2006.

868 Xu, M. N., Li, X., Shi, D., Zhang, Y., Dai, M., Huang, T., Glibert, P. M., and Kao, S.-J.:
869 Coupled effect of substrate and light on assimilation and oxidation of regenerated nitrogen in
870 the euphotic ocean, *Limnol. Oceanogr.*, 64, 1270–1283,
871 <https://doi.org/https://doi.org/10.1002/lno.11114>, 2019.

872 Yin, Q., He, K., Collins, G., De Vrieze, J., and Wu, G.: Microbial strategies driving low
873 concentration substrate degradation for sustainable remediation solutions, *npj Clean Water*, 7,
874 52, <https://doi.org/10.1038/s41545-024-00348-z>, 2024.

875 Yool, A., Martin, A. P., Fernández, C., and Clark, D. R.: The significance of nitrification for
876 oceanic new production, *Nature*, 447, 999–1002, <https://doi.org/10.1038/nature05885>, 2007.

877 Zheng, Z.-Z., Wan, X., Xu, M. N., Hsiao, S. S.-Y., Zhang, Y., Zheng, L.-W., Wu, Y., Zou,
878 W., and Kao, S.-J.: Effects of temperature and particles on nitrification in a eutrophic coastal
879 bay in southern China, *J. Geophys. Res. Biogeosciences*, 122, 2325–2337,
880 <https://doi.org/https://doi.org/10.1002/2017JG003871>, 2017.

881 Zheng, Z.-Z., Zheng, L.-W., Xu, M. N., Tan, E., Hutchins, D. A., Deng, W., Zhang, Y., Shi,
882 D., Dai, M., and Kao, S.-J.: Substrate regulation leads to differential responses of microbial
883 ammonia-oxidizing communities to ocean warming, *Nat. Commun.*, 11, 3511,
884 <https://doi.org/10.1038/s41467-020-17366-3>, 2020.

885 Zhou, Y., Yan, A., Yang, J., He, W., Guo, S., Li, Y., Wu, J., Dai, Y., Pan, X., Cui, D.,
886 Pereira, O., Teng, W., Bi, R., Chen, S., Fan, L., Wang, P., Liao, Y., Qin, W., Sui, S.-F., Zhu,
887 Y., Zhang, C., and Liu, Z.: Ultrastructural insights into cellular organization, energy storage
888 and ribosomal dynamics of an ammonia-oxidizing archaeon from oligotrophic oceans, *Front.*
889 *Microbiol.*, 15, 1367658, <https://doi.org/10.3389/fmicb.2024.1367658>, 2024.

890 Zhu, W., Wang, C., Hill, J., He, Y., Tao, B., Mao, Z., and Wu, W.: A missing link in the
891 estuarine nitrogen cycle? Coupled nitrification-denitrification mediated by suspended
892 particulate matter, *Sci. Rep.*, 8, 2282, <https://doi.org/10.1038/s41598-018-20688-4>, 2018.

893